Appl. Phys. B 81, 517–520 (2005)
DOI: 10.1007/s00340-005-1897-z

Applied Physics B
Lasers and Optics

Y.F. CHEN ✉
Y.S. CHEN
T.H. OU
K.W. SU

Compact efficient diode-pumped Nd:YVO$_4$ Q-switched blue laser with intracavity frequency tripling

Department of Electrophysics, National Chiao Tung University, Hsinchu, Taiwan

Received: 1 February 2005 / Revised version: 14 April 2005

ABSTRACT We demonstrate a compact efficient diode-pumped acousto-optically Q-switched intracavity-frequency-tripled Nd:YVO$_4$ blue laser. The optimum polarization state is experimentally investigated to optimize the output performance. Greater than 280 mW of 447-nm average power at a repetition rate of 25 kHz was generated with a 15-W diode pump power. At 25 kHz, the pulse width is shorter than 15 ns and the peak power is higher than 800 W.

PACS 42.60.Gd; 42.65.Ky; 42.55.Rz

Efficient, compact, high-peak-power, and high-repetition-rate (> 20 kHz) visible-wavelength lasers are of practical importance for many applications such as environmental analysis, spectroscopy and undersea imaging. Diode-pumped solid-state lasers have been shown to be efficient, compact, and reliable all-solid-state optical sources. Frequency doubling of Nd-doped lasers operating at the $4F_{3/2}$–$4I_{9/2}$ transition has been extensively explored during the past few years for producing coherent blue light [1–5]. Another approach for blue laser sources is based on frequency tripling of a Nd-doped laser operating at the $4F_{3/2}$–$4I_{13/2}$ transition [6–10]. Unlike the three-level system of the $4F_{3/2}$–$4I_{9/2}$ transition, stimulated emission at the $4F_{3/2}$–$4I_{13/2}$ transition is a four-level system that can provide a low-threshold and stable laser output due to the lack of sensitive temperature dependence of the transition rate. Up to now, most of the research results involving blue-light generation were focused on the aspects of extracavity third-harmonic generation (THG); the average output power for a blue laser was approximately several tens of milliwatts and the peak power was only up to several tens of watts.

In this work, we demonstrate a compact blue laser by using intracavity THG at 1342 nm in a diode-pumped Q-switched Nd:YVO$_4$ laser. Efficient THG for yielding blue light is achieved by cascading second-harmonic generation (SHG) in a KTP crystal and sum-frequency generation (SFG) in a LBO crystal. At an incident pump power of 15 W, the compact laser cavity, operating at 25 kHz, produces average output powers at 447 nm up to 282 mW and a peak power greater than 800 W.

The experimental configuration for the diode-pumped actively Q-switched blue laser at 447 nm is depicted in Fig. 1. The cavity mirrors have a special dichroic coating for efficient intracavity THG. The input mirror is a 500-mm radius-of-curvature concave mirror with antireflection coating at the pump wavelength (~ 808 nm) on the entrance face ($R < 0.2\%$), high-reflection coating at 1342 nm, 671 nm, and 447 nm ($R > 99.8\%$) and high-transmission coating at the pump wavelength on the other surface ($T > 95\%$). The output coupler has high-reflection coating at 1342 nm and 671 nm ($R > 99.8\%$) and high-transmission coating at 447 nm ($T > 85\%$). Both mirrors have a transmission of 90% at 1064 nm to suppress parasitic oscillations on lines in the 1064-nm region.

The pump source was an 808-nm fiber-coupled laser diode with a core diameter of 800 μm, a numerical aperture of 0.16, and a maximum output power of 16 W. A focusing lens with 12.5-mm focal length and 90% coupling efficiency was used to re-image the pump beam into the laser crystal. The focus radius of the pump beam was around 300 μm. The laser-active medium was a 0.25 at.% Nd:YVO$_4$ crystal with a length of 9 mm. A Nd:YVO$_4$ crystal with a low dopant concentration was used to avoid thermally induced fracture [11]. The laser crystal was placed very near (2–3 mm) to the input mirror. The nonlinear crystal for efficient SHG was a 10-mm-long KTP crystal cut for type-II phase matching at 1342 nm. On the other hand, a sum-frequency mixer for THG was an 8-mm-long LBO crystal cut for type-I phase matching. Both sides of all crystals were coated for antireflection at 1342 nm

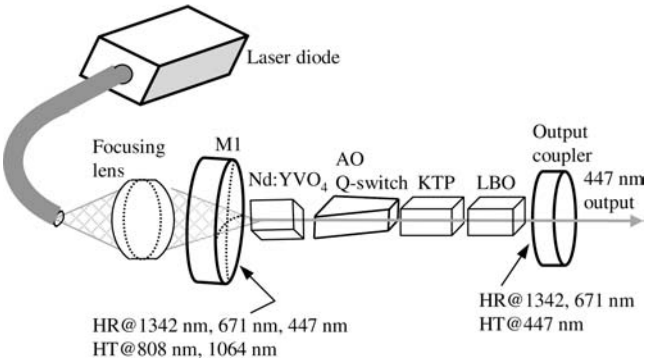

FIGURE 1 Experimental setup for the diode-pumped Q-switched intracavity frequency-tripled blue laser

---

✉ Fax: +886-35-729134, E-mail: yfchen@cc.nctu.edu.tw

and 671 nm ($R < 0.2\%$). The gain medium and nonlinear crystals were wrapped with indium foils and mounted in water-cooled copper blocks. The water temperature was maintained at 25°C. The 20-mm-long acousto-optical Q-switcher (Gooch and Housego) had antireflection coatings at 1342 nm on both faces and was driven at a 40.68-MHz center frequency with 3.0-W of radio-frequency power. The overall laser-cavity length was 65 mm. The spectral information of the laser was monitored by an optical spectrum analyzer (Advantest Q8381A). The spectrum analyzer employing a grating monochromator can be used for high-speed measurement of pulse light with the resolution of 0.1 nm. The pulse temporal behavior was recorded by a LeCroy digital oscilloscope with a fast PIN photodiode.

Since the efficient SHG is of the essence for blue-light generation in SFG, we first investigate the SHG performance in the KTP crystal. For this investigation, only KTP crystal was put into the cavity for the SHG process without LBO crystal. In addition, an output coupler with high-reflection coating at 1342 nm ($R > 99.8\%$) and high-transmission coating at 671 nm ($T > 85\%$) was used instead of the above-mentioned output coupler for THG. For single-pass external type-II SHG, $\varphi = 45°$ can lead to the most effective conversion efficiency, where φ is the angle between the extraordinary axis (E axis) of the KTP crystal and the c axis of the Nd:YVO$_4$ crystal. Note that the angle φ also represents the angle between the polarization of the pump fundamental wave and the polarization of the generated second-harmonic wave. In the intracavity type-II SHG, however, the optimum φ is usually not equal to 45° because the fundamental wave becomes an elliptically polarized wave due to the birefringent effect of the KTP crystal. Based on the experimental results, the optimum φ is found to be approximately 35°. The influence of the polarization effects on the efficiency of intracavity SHG can be analyzed from the theoretical model [12]. The SHG conversion efficiency at $\varphi = 35°$, on the whole, is approximately ten percent higher than that at $\varphi = 45°$. Figure 2 shows the average output power at 671 nm as a function of the incident pump power at a repetition rate of 25 kHz for $\varphi = 35°$. It can be seen that the maximum red output power of 1.08 W was obtained at an incident pump power of 15 W, corresponding to a conversion efficiency of 7.2%. It is worthwhile to mention that the highest average output power at 1342 nm that could be extracted with a proper output coupler ($\sim$ 94% reflectivity at 1342 nm) was about 2.4 W. Accordingly, the maximum second-harmonic power is close to 45% of the available Q-switched fundamental power. Since the following THG is accomplished via a type-I SFM, a smaller φ essentially produces higher conversion efficiency for blue output at 447 nm. Therefore, the configuration with $\varphi = 35°$ is employed for the subsequent intracavity THG experiment.

Since the polarization of the fundamental wave is not parallel to the polarization of the second-harmonic wave, the THG conversion efficiency from type-I SFM strongly depends on the parameter ϑ, where ϑ is the angle between the ordinary axis (O axis) of the LBO crystal and the E axis of the KTP crystal. In general, efficient THG from type-I SFM comes from the power intensities of the fundamental and second-harmonic beams in a ratio of 1:1. In the present configuration, however, the power intensity of the second-harmonic wave is found to be approximately 1.4 times less than that of the fundamental wave. Therefore, the difference of the power intensities between the fundamental and second-harmonic waves for effective SFM can be minimized by setting the O axis of the LBO crystal to be parallel to the polarization of the second harmonic, i.e. $\vartheta = 0°$. Figure 3 depicts the average output power at 447 nm as a function of the incident pump power at a repetition rate of 25 kHz for $\vartheta = 0°$, 15°, and 30°. As

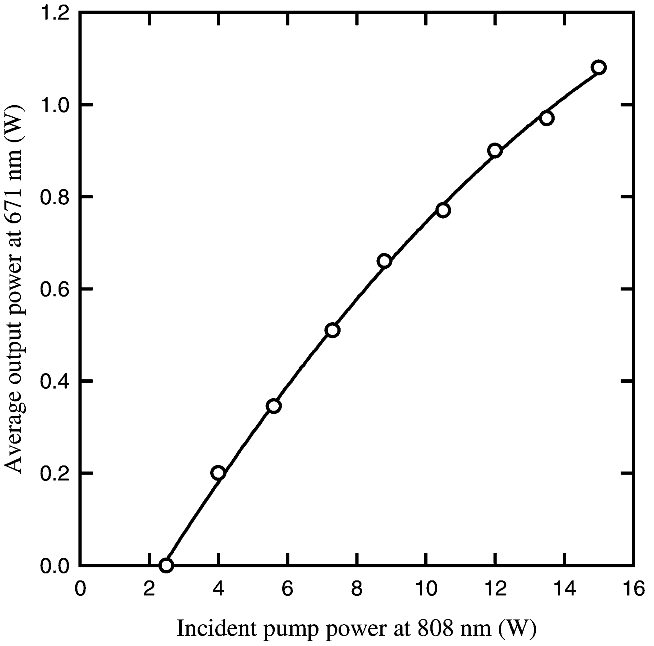

FIGURE 2 The average output power at 671 nm as a function of the incident pump power at a repetition rate of 25 kHz for $\varphi = 35°$, where φ is the angle between the E axis of the KTP crystal and the c axis of the Nd:YVO$_4$ crystal

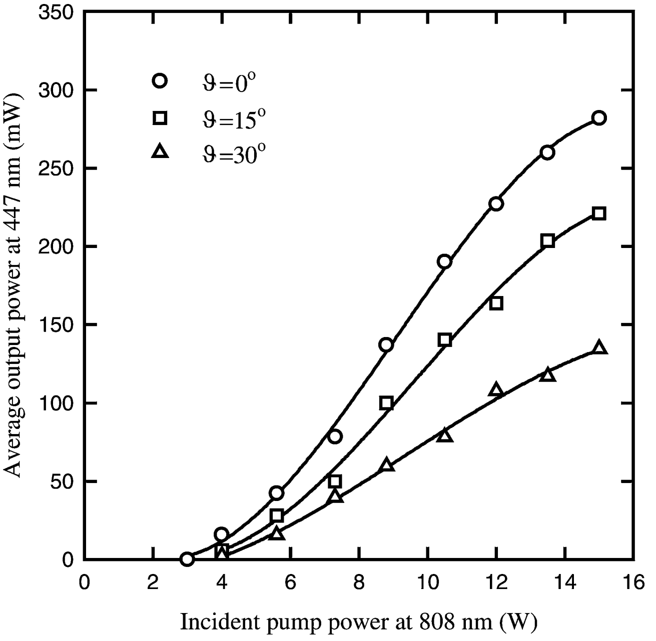

FIGURE 3 The average output power at 447 nm as a function of the incident pump power at a repetition rate of 25 kHz for $\vartheta = 0°$, 15°, and 30°, where ϑ the angle between the O axis of the LBO crystal and the E axis of the KTP crystal

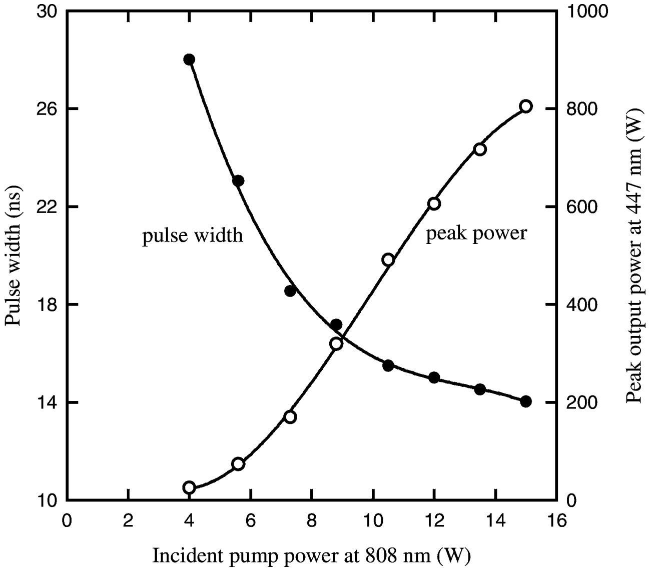

FIGURE 4 The peak blue power and pulse width versus diode pump power at a repetition rate of 25 kHz and $\vartheta = 0°$

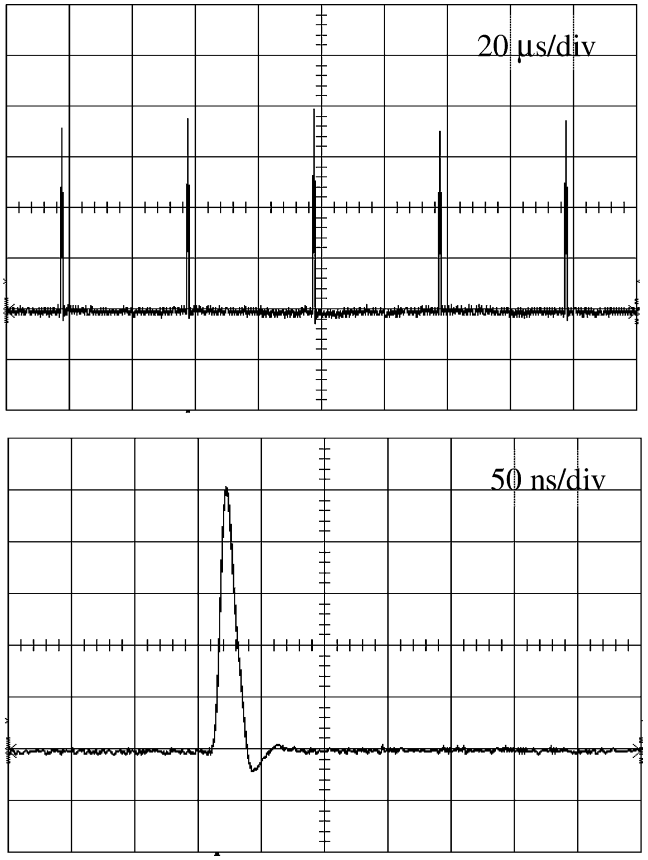

FIGURE 5 Oscilloscope traces of a train of output pulses; the *lower trace* is an expanded shape of a single pulse

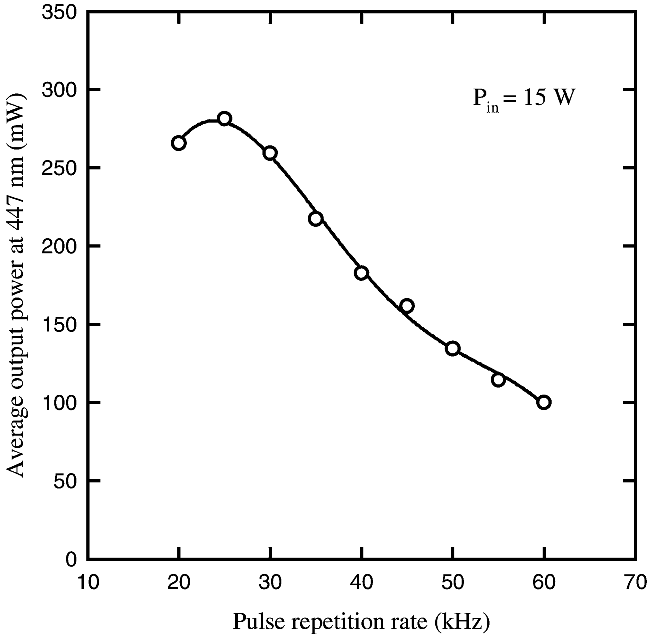

FIGURE 6 The average blue output power at 15 W of pump power as a function of the pulse-repetition rate with the configuration of $\vartheta = 0°$

expected, the average blue output power is highest at $\vartheta = 0°$ and is up to 282 mW at an incident pump power of 15 W, corresponding to a conversion efficiency of 1.9% from pump diode input to blue output. The present result is considerably higher than the output power of ~ 55 mW obtained with extracavity THG [6, 7]. After the optical elements were thermally stabilized, the fluctuations of the average power over hours of operation have been observed to be approximately ±5%. The laser performance was reproducible on a day-to-day basis. With the algorithms of knife-edge technique [13], the beam-quality factor at the maximum output power was estimated to be better than 2.0.

Figure 4 shows the peak blue power and pulse width versus diode pump power at a repetition rate of 25 kHz and $\vartheta = 0°$. The pulse width decreases from 25 ns to 14 ns by increasing the pump power from 5 W to 15 W. The maximum blue peak power amounts to 800 W at 15-W pump power. To our knowledge, this is the highest power ever reported for a diode-end-pumped Q-switched Nd:YVO$_4$ blue laser. The typical output pulse shape is shown in Fig. 5. Figure 6 shows the average blue output power at 15 W of pump power as a function of the pulse-repetition rate with the configuration of $\vartheta = 0°$. To avoid damage to the intracavity optical components, the Q-switcher is operated above 20 kHz. It can be seen that the conversion efficiency falls at a higher repetition rate ($>$ 30 kHz) due to lower power intensities of the fundamental and second-harmonic waves. Even so, the maximum average output power at 447 nm still exceeds 100 mW at a repetition rate of 60 kHz.

We have demonstrated a compact efficient Q-switched Nd:YVO$_4$ blue laser with an intracavity THG scheme. The conversion efficiencies for intracavity SHG and THG were optimized via controlling the polarization state. In the intracavity SHG experiment, 1.08 W of average red output power at a repetition rate of 25 kHz was obtained by setting the *E* axis of the KTP crystal with respect to the *c* axis of the Nd:YVO$_4$ crystal at an incident pump power of 15 W. In the intracavity THG experiment, 282 mW of average blue output power with a 14-ns pulse width at a repetition rate of 25 kHz was generated by setting the *O* axis of the LBO crystal to be along the polarization of the second-harmonic wave at an incident pump power of 15 W. The short pulse width leads to a peak third-harmonic power at 447 nm of up to 800 W.

REFERENCES

1 A. Harada, Y. Nihei, Y. Okazaki, H. Hyuga, Opt. Lett. **22**, 805 (1997)
2 M. Pierrou, F. Laurell, H. Karlsson, T. Kellner, C. Czeranowsky, G. Huber, Opt. Lett. **24**, 205 (1999)
3 W.P. Risk, W. Length, Opt. Lett. **12**, 993 (1987)
4 P. Zeller, P. Peuser, Opt. Lett. **25**, 34 (2000)
5 S. Bjurshagen, D. Evekull, R. Koch, Electron. Lett. **38**, 324 (2002)
6 G.Z. Luo, S.N. Zhu, J.L. He, Y.Y. Zhu, H.T. Wang, Z.W. Liu, C. Zhang, N.B. Ming, Appl. Phys. Lett. **78**, 3006 (2001)
7 X. Mu, W. Shi, Y.J. Ding, J. Appl. Phys. **93**, 9437 (2003)
8 R.A. Stolzenberger, C.C. Hsu, N. Peyghambarian, J.E. Reid, R.A. Morgan, IEEE Photon. Technol. Lett. **1**, 446 (1989)
9 X. Mu, Y.J. Ding, in *Digest of Technical Papers of CLEO 2002* (Optical Society of America, Washington, DC, 2002), paper CtuG3, p. 166
10 G.W. Ross, N.S. Felgate, W.A. Clarkson, P.G.R. Smith, P.E. Britton, D.C. Hanna, in *Digest of Technical Papers of CLEO 1998* (Optical Society of America, Washington, DC, 1998), paper CThN6, p. 384
11 Y.F. Chen, IEEE J. Quantum Electron. **35**, 234 (1999)
12 L. Friob, P. Mandel, E.A. Viktorov, Quantum Semiclass. Opt. **10**, 1 (1998)
13 A.E. Siegman, M.W. Sasnett, T.F. Johnston, Jr., IEEE J. Quantum Electron. **27**, 1098 (1991)